Optical properties of photon echoes stimulated by three frequencies

C. V. Heer and R. L. Sutherland
Department of Physics, Ohio State University, Columbus, Ohio 43210
(Received 12 December 1978)

A gaseous atomic or molecular system with four energy levels $E_a < E_b < E_c < E_d$ which is stimulated by resonant laser pulses at frequencies $\omega_1 \simeq \omega_{ba}$, $\omega_2 \simeq \omega_{cb}$, $\omega_3 \simeq \omega_{dc}$ is considered. The six photon echoes which are stimulated by first and second pulses at frequencies ω_1, ω_2, ω_3 are discussed. For wave fronts which are described by $e^{i(\varphi-\omega t)}$ the echo phase is described by $\varphi_E = \Sigma(2\varphi_m^{II} - \varphi_m^{I})$ at the sum frequency $\omega_1 + \omega_2 + \omega_3$ with $m = 1,2,3$, at $\omega_1 + \omega_2$ with $m = 1,2$, at ω_1 with $m = 1$, etc. For waves in the z direction where $\varphi = \kappa(x,y,z) + kz$ the gradient of the phase yields the wave-vector direction $\vec{k}_E = \Sigma(2\vec{k}_m^{II} - \vec{k}_m^{I})$ in a physically thin sample. A probe pulse at ω_2 and ω_3 after the second pulse can generate a probe-pulse echo at ω_1 with phase $\varphi_1 = \Sigma(2\varphi_m^{II} - \varphi_m^{I}) - \varphi_2^S - \varphi_3^S$, etc., for other frequency arrangements. Transverse phases $\kappa_m(xy)$ can be added and subtracted, but no application is suggested for this novel feature. When all κ_m except one are zero, phase conjugation or phase-adaptive optics can occur.

I. INTRODUCTION

Recent development in quantum optics and nonlinear optics have provided methods for manipulating the phase of light waves. Phase-adaptive optics[1,2] and phase conjugation[3,4] are recent applications.[5,6] Parametric image conversion was an earlier application.[7] Although some aspects of holography occur on a short time scale, nonlinear optics can provide additional optical effects. Many of these nonlinear effects are due to coherent space-phase information which is stored in the off-diagonal density-matrix elements and can become observable via the electric polarization. This paper examines some of the optical characteristics of the waves formed by laser radiation at frequencies ω_1, ω_2, ω_3 interacting in a nonlinear medium. Resonant interaction with the four states a, b, c, d which are shown in Fig. 1 are given primary consideration and hence include optical nutation, free-induction decay, and photon echoes.

A simple example for photon echoes shows that for thin samples the radius of curvature z_E of the echo at the sum frequency $\omega_E = \omega_1 + \omega_2 + \omega_3$ is related to the radii of curvature of the first and second pulses by

$$\frac{1}{z_E} = \sum \left(\frac{\omega_n}{\omega_E}\right)\left(\frac{2}{z_n^{II}} - \frac{1}{z_n^{I}}\right) .$$

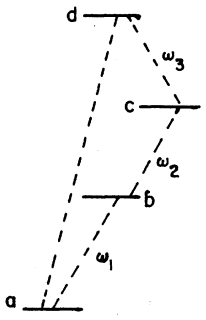

FIG. 1. States a, b, c, d and the near-resonant frequencies ω_1, ω_2, ω_3 are defined in this figure. ab, bc, cd, ad are electric dipole transitions and ac, bd are electric quadrupole transitions.

For more general wave fronts the space phases φ of the eikonal $e^{i(\varphi-\omega t)}$ can be added and subtracted. A new pulse at a new frequency can be formed which depends on the product of the electric fields of the stimulating waves. Thin samples provide a large number of possible arrangements and as the samples become thicker this number is reduced by phase-matching restrictions. Although $e^{i(\varphi-\omega t)}$ can be formed where φ is a sum of the various space phases of the interacting waves, it is not clear that this necessarily provides useful optical information. This is apparent for the simple single-frequency photon echoes.[4,8] It is possible to change a wave $e^{i\kappa}e^{i(k_z-\omega t)}$ into $e^{i2\kappa}e^{i(kz-\omega t)}$ and for a single point source this changes the apparent radius of curvature by a factor of 2. For a more general wave $ve^{i\kappa} = \sum e^{i\kappa_m}$, where $e^{i\kappa_m}$ describes a spherical wave with origin m in the object plane, the new wave front $v^2 e^{i2\kappa} = (\sum e^{i\kappa_m})^2$ becomes quite complex. A new virtual source is formed for each pair of source points in the object plane. This can be compared with the echo experiment[4] in which $ve^{i\kappa}$ is changed into $ve^{-i\kappa}$ and the superposition principle applies. Information is contained in both the amplitude v and the phase $e^{i\kappa}$. In forming the nonlinear product $v_1 v_2 v_3\, e^{i(\kappa_1+\kappa_2+\kappa_3)}$ it will be shown in subsequent sections that the phases can be modified. The conjugate $e^{-i\kappa}$ can be formed experimentally if 1 and 2 are plane waves so that v_1 and v_2 are constants and $\kappa_1 = \kappa_2 = 0$, then superposition can be used. Examples of this type are discussed. For the resonant phenomena discussed

in this paper more important examples have almost constant amplitudes across the wave fronts. This corresponds to radiation which originates from three real or virtual point sources and which is subsequently phase deformed. In this sense each wave corresponds to the eikonal expansion in which almost all the optical information is in the phase.

Three-wave resonant effects are considered since the sum frequency is an allowed electric dipole transition for gases, isotropic liquids, and cubic solids. Earlier developments have considered two-wave effects, and, since the allowed electric quadrupole effects are weak, the observations have been made usually by probe radiation.

If the density matrix element is denoted by σ_{mn} for a molecule in the sample, a common feature for all these coherent phenomena is that $\langle \sigma_{mn} e^{-i\psi_a} \rangle$ can be of the order of unity for excitation by coherent waves as the average is taken over position and velocity. A new wave $e^{i\psi}$ is generated and ψ_a denotes the value of the eikonal at the molecular position. Thus excitation by three waves at frequencies ω_1, ω_2, ω_3 stimulates electric dipole transition waves at the sum frequency $\omega_1+\omega_2+\omega_3$ via $\langle \sigma_{da} e^{-i\psi} \rangle$; at ω_1 via $\langle \sigma_{ba} e^{-i\psi_1} \rangle$; at ω_2 via $\langle \sigma_{cb} e^{-i\psi_2} \rangle$; and at ω_3 via $\langle \sigma_{dc} e^{-i\psi_3} \rangle$. $\langle \sigma_{ca} e^{-i\psi_{12}} \rangle$ and $\langle \sigma_{db} e^{-i\psi_{23}} \rangle$ also have macroscopic values, but are observable only in the quadrupole approximation. These coherent density-matrix elements occur for the resonant interactions, that is as optical nutation for laser radiation which is turned on suddenly, as free-induction decay when the radiation is turned off, and as photon echoes for multiple pulses. Even after a pulse is turned off quantities like $\sigma_{da}(t)$ persist until destroyed by relaxation mechanisms. Thus if a pulse is turned off at t_1 as shown in Fig. 2 and probe pulses are applied at ω_1 and ω_2 then $\sigma_{da}(t_1)$ with its inherent phases in exp $i\psi(t_1)$ can be used to generate a new wave at ω_3. If a probe pulse is applied at ω_2 then $\sigma_{ca}(t_1)$ with its inherent phase has the spatial coherence of a traveling wave and generates a new wave at ω_1. For two-wave radiation or two-photon effects, probe radiation has been used to make the effects observable.[9] Probe radiation was used to observe the spin-flip Raman echo[10] in n-type CdS; to observe the two-photon echo in Na vapor[11]; and to observe two-photon optical free-induction decay[12] in Na vapor.

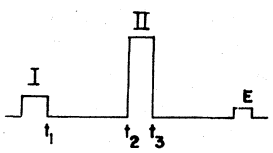

FIG. 2. First set of pulses I at frequencies ω_1, ω_2, ω_3 occur during interval t_1-0 and the second set of pulses II occur during t_3-t_2. The photon echoes occur near t_E-t_3=t_2-t_1.

Focusing of single-wave photon echoes[4] and phase conjugation[3] has been suggested and has been observed recently.[6] This phenomenon is observed in the forward direction for conventional echoes, optical nutation, and free-induction decay. These are all pulse phenomena. Steady-state effects can be observed and have the wave front characteristics of optical nutation or free-induction decay. Three-wave mixing at a single frequency $\omega_1=\omega_2=\omega_3$ and on a single transition has been used recently for phase-adaptive optics.[1,2] Only the pair of states a and b are used in Fig. 1, but the waves travel in different directions. If two saturating waves $e^{i(kz-\omega t)}$ and $e^{-i(kz+\omega t)}$ and a signal wave $ve^{-i(\varphi-\omega t)}$ are superimposed in the nonlinear medium, a counterpropagating wave $v'e^{i(\varphi+\omega t)}$ is generated by σ_{ba}. This type of phase-adaptive optics has been observed in such nonlinear media[5] as liquid CS_2, Na vapor, and Ge.

The theory developed in this paper is primarily for physically thin gaseous samples where the index of refraction is not important. As the sample becomes thicker the index of refraction cannot be neglected. Since pulsed resonant transitions are considered the indices of refraction for the three frequencies are not clearly defined. This may introduce an experimental problem for thick samples.

II. THEORY

A. General theory

The theory of four-level resonant interaction is considered first. For simplicity the atomic or molecular states are denoted by a, b, c, d, and when necessary the state $|a)$ implies the quantum numbers $|aJ_am_a)$, etc. An energy-level diagram is shown in Fig. 1. An electric dipole interaction $V(t)=-\vec{P}\cdot\vec{E}(t)$ is used and the Hamiltonian in the rotating-wave approximation can be written

$$H=H_0+V(t)\,, \tag{1a}$$

with

$$V(t)=\hbar[|b)(a|v_1e^{i\psi_1}+|c)(b|v_2e^{i\psi_2}+|d)\times(c|v_3e^{i\psi_3}+\text{H.c.}]. \tag{1b}$$

The eikonal phase

$$\psi_n=\varphi_n+(\dot{\varphi}_n-\omega_n)t\,, \tag{2a}$$

and where $n=1,2,3$ and

$$\hbar v_1=(b|\vec{P}|a)\cdot\hat{u}_1E_1\,, \tag{2b}$$

etc., for v_2 and v_3. Bracket notation is used and $(b|a)=\delta_{ab}$. The eikonal approximation is used and for a molecule at position $\vec{r}_\alpha(t)$ the space phase $\varphi[\vec{r}_\alpha(t)]$ in the absence of collisions can be written $\varphi+\dot{\varphi}\,t$. φ_n is the phase at the initial position $\vec{r}_\alpha(0)$ and the Doppler shift is given by

$$\dot{\phi}=(\mathrm{grad}\varphi)\cdot\dot{\vec{r}}_\alpha\,. \tag{2c}$$

$\hat{u}_1$ is the polarization and E_1 the amplitude of the laser field at frequency ω_1. If the operator $A(t)$ is introduced where

$$A(t)=e^{i\delta} \tag{3a}$$

and

$$\delta=\psi_1|b)(b|+(\psi_1+\psi_2)|c)(c|+(\psi_1+\psi_2+\psi_3)|d)(d|\,, \tag{3b}$$

the interaction $V(t)$ becomes time independent

$$V_I=A^\dagger(t)V(t)A(t)\,. \tag{4}$$

The transformed Schrödinger equation can be integrated for a constant $\dot{\delta}$. With ξ defined as

$$\xi=\hbar^{-1}(H_0+V_I)+\dot{\delta}\,, \tag{5}$$

the time evolution of the system is described by

$$U(t,t_m)=A(t)e^{-i\xi(t-t_m)}A^\dagger(t_m)\,. \tag{6}$$

Discontinuous or abrupt changes in either v_n or $\dot{\psi}_n$ can be treated with this unitary matrix. The position of $A^\dagger(t_m)$ keeps the phase correct.

With $E_a=0$ and with the notation for off resonance

$$\Delta_1=\omega_{ba}-\omega_1+\dot{\varphi}_1\,, \tag{7a}$$

$$\Delta_2=\omega_{ca}-\omega_1-\omega_2+\dot{\varphi}_1+\dot{\varphi}_2\,, \tag{7b}$$

etc., for Δ_3, ξ can be written in matrix form as

$$\xi=\begin{bmatrix}0 & v_1^* & 0 & 0\\ v_1 & \Delta_1 & v_2^* & 0\\ 0 & v_2 & \Delta_2 & v_3^*\\ 0 & 0 & v_3 & \Delta_3\end{bmatrix}\,, \tag{8}$$

and the states are labeled a, b, c, d for rows and columns. Matrix elements of $e^{i\xi t}$ can be found by finding the roots λ_k of the ξ matrix and then by using the expansion theorem

$$e^{i\xi t}=\sum_k e^{i\lambda_k t}\prod_{k\neq l}\left(\frac{\xi-\lambda_l}{\lambda_k-\lambda_l}\right). \tag{9}$$

The essential features for the formation of photon echoes can be discussed by considering resonance and making all $\Delta_n=0$. For real v_n the four roots follow from

$$\lambda_\pm^2=\tfrac{1}{2}(v_1^2+v_2^2+v_3^2)\pm[\tfrac{1}{4}(v_1^2+v_2^2+v_3^2)^2-v_1^2v_3^2]^{1/2}\,, \tag{10}$$

where $\lambda_{++}=-\lambda_{-+}=\lambda_+$ and $\lambda_{--}=-\lambda_{+-}=\lambda_-$. Direct use of the expansion theorem yields,

$$e^{i\xi t}=(\lambda_+^2-\lambda_-^2)^{-1}[\,(\lambda_+^2\cos\lambda_- t-\lambda_-^2\cos\lambda_+ t)-i\xi(\lambda_-^2\lambda_+^{-1}\sin\lambda_+ t-\lambda_+^2\lambda_-^{-1}\sin\lambda_- t)$$
$$+\xi^2(\cos\lambda_+ t-\cos\lambda_- t)+i\,\xi^3(\lambda_+^{-1}\sin\lambda_+ t-\lambda_1^{-1}\sin\lambda_- t)\,]\,; \tag{11}$$

ξ^2 and ξ^3 follow from Eq. (8) by matrix multiplication.

Evolution in time of the density matrix for a molecule at position $\vec{r}_\alpha$ follows from

$$\sigma_\alpha(t)=[U(t,t_0)\sigma(t_0)U^\dagger(t,t_0)]_\alpha\,, \tag{12}$$

and the electric dipole moment of the radiating molecule is

$$\vec{d}_\alpha=\mathrm{Tr}\vec{P}\sigma_\alpha(t)\,. \tag{13}$$

Thus the quantity of primary interest for echo formation at the sum frequencies is

$$\sigma_{da}(t)=(d|\sigma_\alpha(t)|a)\,. \tag{14}$$

The electric field generated by these oscillating dipoles follows in the usual manner,[4,8] and with the brackets $\langle\ \rangle$ denoting an average over molecular positions and velocities

$$\vec{E}_E(\vec{r},t)=(i\pi Nlp/\epsilon_0\lambda)\langle\sigma_{da}e^{-i\psi_{E\alpha}}\rangle \times e^{i(\varphi_E-\omega_E t)}+\mathrm{c.c.}, \tag{15}$$

where σ_{da} and $\psi_{E\alpha}$ are evaluated at $\vec{r}_\alpha(t)$, N is the number of molecules/m^3, l is the sample length, λ is the wavelength, and $p=(a|P|d)$. Since the pulse amplitude is reduced to zero between pulses, it is convenient to introduce the evolution operator

$$U_0(t,t_m)=e^{-iH_0(t-t_m)/\hbar}\,. \tag{16}$$

The matrix elements for the density matrix which is given by Eq. (12) are relatively simple even for multiple pulses at resonance. Off-res-

onance numerical solutions follow in a direct manner. A single damping constant can be introduced by allowing all density-matrix elements to decay as $e^{-\gamma t}$. A more correct theory with different damping constants for off-diagonal and diagonal density-matrix elements requires the same degree of sophistication as the two-level problem.[13] The 4×4 density matrix must be converted to a 1×16 column matrix and these column matrices are then related by a 16×16 matrix. Although greater detail is included in this "vector model," there is a loss of clarity and only numerical solutions can be obtained.

B. Photon echoes at $\omega_E = \omega_1 + \omega_2 + \omega_3$

For the two-pulse sequence which is shown in Fig. 2, the time evolution σ_{da} follows from Eq. (11) with

$$U(t,0) = U_0(t,t_3)U_{\rm II}(t_3,t_2)\,U_0(t_2,t_1)U_{\rm I}(t_1,0). \quad (17)$$

Of the many terms which contribute to σ_{da} the photon echo depends on

$$\sigma_{da}(t) = e^{i\Psi_{E\alpha}} f_{da}, \quad (18)$$

where the amplitude

$$f_{da} = (d|e^{-i\xi_{\rm II}\tau_{\rm II}}|a)(a|e^{-i\xi_{\rm I}\tau_{\rm I}}|a) \times (a|e^{i\xi_{\rm I}\tau_{\rm I}}|d)(d|e^{i\xi_{\rm II}\tau_{\rm II}}|a), \quad (19a)$$

and the eikonal phase

$$\Psi_{E\alpha} = -\omega_{da}(t - t_3 - t_2 + t_1) + \sum_n [\psi_n^{\rm II}(t_3) + \psi_n^{\rm II}(t_2) - \psi_n^{\rm I}(t_1)], \quad (19b)$$

where $\omega_{da} = (E_d - E_a)/\hbar$. The time intervals $\tau_{\rm I} = t_1 - 0$ and $\tau_{\rm II} = t_3 - t_2$, and $\xi_{\rm I}$ and $\xi_{\rm II}$ use the values of $\Delta_{n\alpha}$ and $v_{n\alpha}$ which are appropriate for the first and second pulses for the molecule at $\vec{r}_\alpha(t)$. In the absence of collisions the eikonal can be written in the form which is given by Eqs. (2a) and (2c). Since the initial position $\vec{r}_\alpha(0)$ and the velocity $\dot{\vec{r}}_\alpha$ are statistically independent variables the average over position and velocity can be taken separately in Eq. (15). As the average over initial molecular positions is taken,

$$\langle \sigma_{da} e^{-i\psi_{E\alpha}} \rangle = \langle e^{i(\Psi_{E\alpha} - \psi_{E\alpha})} f_{da} \rangle, \quad (20)$$

the average is large when the geometrical optics of the echo is described by

$$\varphi_E = \sum_n (2\varphi_n^{\rm II} - \varphi_n^{\rm I}). \quad (21a)$$

This implies that the Doppler term for the molecule with velocity $\dot{\vec{r}}_\alpha$ is

$$\dot{\varphi}_{E\alpha} = \sum_n (2\dot{\varphi}_n^{\rm II} - \dot{\varphi}_n^{\rm I})_\alpha. \quad (21b)$$

With these definitions of φ_E and $\dot{\varphi}_{E\alpha}$ and

$$\Delta_{E\alpha} = -(\omega_{da} - \omega_E + \dot{\varphi}_{E\alpha}), \quad (21c)$$

the average over only molecular velocities can be written as

$$\langle \sigma_{da} e^{-i\psi_{E\alpha}} \rangle = \langle e^{i\Delta_{E\alpha}(t - t_3 - t_2 + t_1)} e^{i\epsilon_\alpha} f_{da} \rangle. \quad (22)$$

At time $t - t_3 = t_2 - t_1 = \tau$ the average is independent of the Doppler effect $\Delta_{E\alpha}$ and is the usual condition for an echo at interval T after the second pulse.

The direction of the wave vector for arbitrary $\vec{r}$ is given by

$$\vec{k}_E = \mathrm{grad}\varphi_E \quad (23)$$

For nonparallel plane waves the echo direction follows from

$$\vec{k}_E = 2(\vec{k}_1^{\rm II} + \vec{k}_2^{\rm II} + \vec{k}_3^{\rm II}) - (\vec{k}_1^{\rm I} + \vec{k}_2^{\rm I} + \vec{k}_3^{\rm I}), \quad (24)$$

and some of the many interesting features which can occur are discussed in a subsequent section.

There remains a phase term

$$\epsilon_\alpha \cong \sum_n (\dot{\varphi}_n^{\rm II} - \dot{\varphi}_n^{\rm I})(t_3 + t_2) \quad (25)$$

which limits the angle between the first and second set of pulses. This is the dominant term and the coefficient of t_1 has been omitted. A thermal average $\langle e^{i\epsilon} \rangle$ over molecular velocities yields a decay[8] $\exp[-\pi(\pi\theta\bar{v}T/\lambda)^2]$, where T is the interval and θ is a typical angle between pulse directions. This yields the most rapid decay and other terms in the average can decrease the decay rate.

The optimum pulse amplitude and direction depends on the matrix elements which follow from Eq. (11)

$$(d|e^{i\xi\tau}|a) = i(v_1v_2v_3)(\lambda_+^2 - \lambda_-^2)^{-1} \times [\lambda_+^{-1}\sin\lambda_+\tau - \lambda_-^{-1}\sin\lambda_-\tau], \quad (26a)$$

and

$$(a|e^{i\xi\tau}|a) = (\lambda_+^2 - \lambda_-^2)^{-1}[\lambda_+^2\cos\lambda_-\tau - \lambda_-^2\cos\lambda_+\tau + v_1^2(\cos\lambda_+\tau - \cos\lambda_-\tau)]. \quad (26b)$$

The influence of the first pulse depends on the product of these two matrix elements and the influence of the second pulse depends on the absolute square of Eq. (26a). An optimum choice of the pulse strength $\lambda\tau$ is no longer the conventional $2\lambda_{\rm I}\tau_{\rm I} = \pi/2$ and $2\lambda_{\rm II}\tau_{\rm II} = \pi$ for the two-level system. Furthermore the dependence on the three laser intensities permits many options. If equal amplitudes for the interaction are selected, that is $v_1 = v_2 = v_3$ then the roots are $\lambda_\pm^2 = \frac{1}{2}(3 \pm 5^{1/2})v^2$. A simple choice is considered. Let $2\lambda_-\tau = \frac{1}{2}\pi$ for

the first pulse and π for the second pulse and then

$$(d|e^{i\xi_T}|a) = +i\ 0.27 \text{ or } +i\ 0.95, \tag{27a}$$

$$(a|\ e^{i\xi_T}|a) = +0.38 \text{ or } \cdots\ , \tag{27b}$$

where the first value of each matrix element is for a $\frac{1}{2}\pi$ pulse and the second value for a π pulse. This sequence yields an echo amplitude of 0.10 and as off-resonance terms are considered should be a good choice. Even so the intensity will be 0.02 of that for the usual two-level echo.

C. Photon echoes at ω_1, ω_2, and ω_3

There are photon echoes at frequencies ω_1, ω_2, and ω_3 which occur simultaneously with the sum-frequency echo discussed in the previous section. Echoes at these frequencies are generated by the electric dipole moments which are due to σ_{ba} for ω_1, σ_{cb} for ω_2, and σ_{dc} for ω_3. Direct evaluation of the density-matrix element for the echo at ω_1 yields

$$\sigma_{ba} = e^{i\Psi_{E\alpha}} f_{ba}\ , \tag{28}$$

where f_{ba} is given by Eq. (19a) with d replaced by b. With $n=1$ $\Psi_{E\alpha}$ is given by Eq. (19b) with ω_{ba}, φ_E by Eq. (21a), $\dot{\varphi}_{E\alpha}$ by Eq. (21b), and $\Delta_{E\alpha} = -(\omega_{ba} - \omega_1 + \dot{\varphi}_{E\alpha})$. The geometrical optics of the echo is described by

$$\varphi_E = 2\varphi_1^{II} - \varphi_1^{I}\ , \tag{29}$$

and the focusing effects for such a pulse sequence has been discussed and observed[6] for a single pair of levels.

At frequency ω_2 the echo is generated by

$$\sigma_{cb} = e^{i\Psi_{E\alpha}} f_{cb}\ , \tag{30}$$

where f_{cb} is given by Eq. (19a) with the state sequence *daaaadda* replaced by *cbbaaccb*. $n=2$ in Eq. (19b) for $\Psi_{E\alpha}$ and the discussion is similar to that for σ_{ba} with $n=1$ replaced by $n=2$, i.e., $\varphi_E = 2\varphi_2^{II} - \varphi_2^{I}$. At frequency ω_3 the echo is generated by

$$\sigma_{dc} = e^{i\Psi_{E\alpha}} f_{dc}, \tag{31}$$

where the state sequence for f_{dc} in Eq. (19a) is *dccaaddc* and $n=3$ is used throughout.

These echoes differ from the usual two-level echoes in the product of the matrix elements and therefore only in the echo intensity. For equal v_n and the pulse strengths which were used for Eq. (27), the echo at ω_2 is 100 times more intense than the sum-frequency echo $\omega_1+\omega_2+\omega_3$. The echoes at ω_1 and ω_3 are 0.02 of the sum echo. A small change in the pulse strength can quite easily change these ratios and can even reverse them. Also as molecules of off-resonance are averaged to form the echo, these terms will be less sensitive to the value selected for the pulse strength.

D. Photon echo at $\omega_1+\omega_2$ and $\omega_2+\omega_3$

There are density-matrix elements σ_{ca} and σ_{db} which have the correct features to produce an echo at the sum frequencies $\omega_1+\omega_2$ and $\omega_2+\omega_3$. These matrix elements have the typical form of Eq. (18). f_{ca} is formed by the state sequence *caaaacca* and f_{db} by *dbbaaddb* in Eq. (19a). $\Psi_{E\alpha}$ and the subsequent discussion uses $n=1$ and 2 for σ_{ca} and $n=2$ and 3 for σ_{db}. The geometrical optics are described by

$$\varphi_E = 2(\varphi_1^{II} + \varphi_2^{II}) - (\varphi_1^{I} + \varphi_2^{I})\ , \tag{32}$$

for $\omega_E = \omega_1 + \omega_2$ and with subscripts 2 and 3 for $\omega_E = \omega_2 + \omega_3$.

Even though macroscopic coherence occurs for the density-matrix elements they are not observable in the electric dipole approximation. If the electric dipole which is stimulated by $\mathrm{Tr}\,\vec{P}e^{i\vec{k}\cdot\vec{r}}\sigma$ is considered, then the quadrupole matrix elements $(c|\vec{D}\cdot\vec{k}|a)$ and $(d|\vec{D}\cdot\vec{k}|b)$ are nonzero and generate an echo. This echo will be quite weak.

E. Focusing, phase conjugation, and related effects

Let the phase of a spherical wave $\varphi = kr = \mu(\omega/c)\,r$, where μ is the index of refraction and then for an almost plane wave in the z direction use the Fresnel approximation

$$\varphi(x,y,z) = \left(\frac{\mu\omega}{c}\right)\left((z-z_0) + \frac{(x-x_0)^2 + (y-y_0)^2}{2(z-z_0)}\right)\ , \tag{33}$$

for a center of curvature at x_0, y_0, z_0. Direct substitution of this approximation into Eq. (21a) yields the phase of the echo in terms of the known centers of curvature x_n^I, y_n^I, etc. For gases or vapors it is convenient to let the index of refraction $\mu = 1+\delta$, where δ is usually less than 10^{-4}. The gradient of Eq. (21a) yields the wave-vector direction and for a thin sample located near $z=0$, and the coefficient of x^2 in Eq. (21a) or $\hat{x}x$ in its gradient can be used to show that

$$\frac{1}{z_E} = \sum_n \left(\frac{\omega_n}{\omega_E}\right)\left(\frac{2}{z_n^{II}} - \frac{1}{z_n^{I}}\right)\ , \tag{34}$$

where $n=1,2,3$. z_E is the radius of curvature of the echo at $z=0$ in terms of the radii of curvature of the wave fronts in the first pulse z_n^I and the second pulse z_n^{II}. In forming the average over position in Eq. (20) this choice of z_E makes the phase independent of x_α^2 and y_α^2. The location of the off-axis center of curvature follows from

either the coefficient of x in Eq. (21a) or from $\hat{x}\cdot$grad of this phase equation and

$$\frac{x_E}{z_E}=\sum_n\left(\frac{\omega_n}{\omega_E}\right)\left(\frac{2x_n^{II}}{z_n^{II}}-\frac{x_n^{I}}{z_n^{I}}\right). \tag{35}$$

If the centers of curvature do not lie in the same plane there is a similar equation for y_E. Equation (35) is one of the usual phase-matching conditions for small δ and for centers of curvature in the x plane, $\theta_n=x_n/z_n$. The dependence of the phase in Eq. (20) on x_α is removed by Eq. (35) for thin samples.

As the sample becomes thicker there is distortion introduced as one replaces z_E by z_E-z in Eq. (34). A more important effect is the z-dependence of the phase or $\hat{z}\cdot$grad and this phase matching condition is

$$\eta=\sum_n\left(\frac{\omega_n}{c}\right)\left[(\delta_E-\delta_n)-\tfrac{1}{2}\theta_E^2+(\theta_n^{II})^2-\tfrac{1}{2}(\theta_n^{I})^2\right]. \tag{36}$$

For planar optics $\theta_n\cong x_n/z_n$ and more generally $\theta_n^2\cong(x_n^2+y_n^2)/z_n^2$. Again in the average over position in Eq. (20) the phase becomes independent of z_α for $\eta=0$. For $\eta l>1$, where l is the sample thickness cancellation of the echo begins to occur as ηl grows. Since the radiation is near resonance there is some difficulty in knowing the index of refraction in even the low-density vapor. A thickness estimate can be made by choosing $\theta^2 l/\lambda<1$.

For more general waves the echo wave front in the medium $v_E e^{i\varphi_E}$ is used with Kirchoff's formulation of Huygens principle and the Fresnel approximation to find the wave front at subsequent positions along the z axis.

F. Generation of a new pulse by $\sigma_{da}(t')$ for a probe pulse at $t'>t_3$

If a signal is applied at the time t' after the second pulse, the change in the density matrix is given by

$$\sigma(t)=U_S(t,t')\sigma(t')U_S^{\dagger}(t,t'). \tag{37}$$

Consider first the radiation generated by $\sigma_{da}(t')$ which is given by Eq. (18). Direct substitution for σ_{ba} yields

$$\sigma_{ba}=e^{i\Psi_\alpha}(b|e^{-i\xi s(t-t')}|d)\,f_{da}(a|e^{i\xi s(t-t')}|a), \tag{38}$$

where

$$\Psi_\alpha=\psi_1^S-\sum_n[\psi_n^S(t')-\psi_n^{II}(t_3)-\psi_n^{II}(t_2)+\psi_n^{I}(t_1)]-\omega_{da}(t'-t_3-t_2+t_1). \tag{39a}$$

The arguments used for Eqs. (20)–(22) can be repeated. The phase φ_1 follows from

$$\varphi_1=\varphi_1^S-\sum_n(\varphi_n^S-2\varphi_n^{II}+\varphi_n^{I}), \tag{39b}$$

and implies a Doppler effect of

$$\dot{\varphi}_{1\alpha}=\dot{\varphi}_{1\alpha}^S-\sum(\dot{\varphi}_n^S-2\dot{\varphi}_n^{II}+\dot{\varphi}_n^{I})_\alpha. \tag{39c}$$

Equation (15) can be repeated and the amplitude of the wave $e^{i(\varphi_1-\omega_1 t)}$ is proportional to the average over molecular velocities of $\langle\sigma_{ba}e^{-i\psi_{1\alpha}}\rangle$. With Eqs. (38) and (39)

$$\Psi_\alpha-\psi_{1\alpha}=-\Delta_\alpha(t'-t_3-t_2+t_1)+\epsilon_\alpha,$$

where

$$\Delta_\alpha=\omega_{da}-\omega_1-\omega_2-\omega_3+\sum\dot{\varphi}_n^S.$$

For radiation with amplitudes v_2^S and v_3^S at frequencies ω_2 and ω_3 and applied at time t', a wave is generated at frequency ω_1 with phase φ_1 even though the amplitude $v_1^S=0$. The radiation at ω_1 with phase φ_1 even though the amplitude $v_1^S=0$. The radiation at ω_1 occurs for $t'-t_3=t_2-t_1$ or t' at the time of the echo. The radiation at ω_1 persists for a time which is dependent on the time interval $t-t'$ and the average over $\dot{\varphi}_\alpha$ emphasizes a select group of velocities such that the decay interval is similar to that for free induction decay.

It should be noted that v_1^S and φ_1^S could have been omitted, but the notation is less cumbersome and $v_1^S=0$ can be introduced at the end of the formulation. The bd matrix element of Eq. (38) depends on ξ^2, or on the product $v_2^S v_3^S$ and determines the amplitude of the effect. At resonance Eq. (11) can be used, but with $v_1^S=0$ it should be noted that $\lambda_+^2\xi=\xi^3$, etc. Again unusual phase or focusing effects occur for these new waves. For spherical waves Eq. (33) can be used with Eq. (39b) to determine the focusing effect for thin samples or the phase-matching conditions for thick samples.

The off-diagonal density-matrix elements $\sigma_{ca}(t')$ can generate new signals. If f_{da} in Eq. (38) is replaced by f_{ca} which is described in Sec. II D, radiation with amplitude v_2^S at frequency ω_2 generates a wave with phase φ_1 at frequency ω_1 via σ_{ba}. The sum in Eq. (39) is over $n=1$ and 2. Radiation at frequency ω_1 generates a wave with φ_2 and ω_2 via σ_{cb}. In a similar manner $\sigma_{db}(t')$ or f_{db} when stimulated by radiation at ω_3 generates a wave at frequency ω_2 via σ_{cb}, and when stimulated by ω_2 generates a wave at ω_3 via σ_{dc}. The focusing effect for thin samples and phase matching for thick samples follow from the gradient of Eq. (39b) with suitable pairs of values for n.

G. Optical nutation and free-induction decay

For completeness optical nutation and free-induction decay are included in the notation of this paper. Optical nutation occurs after the radiation is turned on at the three frequencies and optical nutation can occur for all frequency combinations. At the sum frequency $\omega_N = \omega_1 + \omega_2 + \omega_3$, one has

$$\sigma_{da}(t) = (d|e^{-i\xi t}|a)(a|e^{i\xi t}|a)e^{i\Psi_{N\alpha}}, \tag{40}$$

where $\Psi_{N\alpha} = \sum \psi_n(t)$. The modulation or nutation is due to the matrix element terms as the average over $\dot{\varphi}_\alpha$ is taken. The phase of the coherent wave generated by σ_{da} is

$$\varphi_N = \sum_n \varphi_n . \tag{41a}$$

Phase matching is necessary for a thick sample and for plane waves $\vec{k}_N = \vec{k}_1 + \vec{k}_2 + \vec{k}_3$ is required. For a thin sample one has for spherical waves

$$\frac{1}{z_N} = \sum_n \left(\frac{\omega_n}{\omega_N}\ \frac{1}{z_n}\right). \tag{41b}$$

Thus for thin samples the wave front of the sum frequency is directly related to the sum of the wave fronts for the three stimulating waves.

Optical nutation at frequency ω_1 is given by σ_{ba} which may be obtained from Eq. (40) by replacing d with b and a $\Psi_{N\alpha}$ which depends on φ_1 and ω_1. This differs from the two level nutation in that the roots λ_k depend on all amplitudes v_n. Similar arguments apply to σ_{dc} for ω_3 and σ_{cb} for ω_2.

There is also a coherent excitation generated by σ_{db} at frequency $\omega_2 + \omega_3$ and σ_{ca} at $\omega_1 + \omega_2$, but only quadrupole nutation can be observed.

Free-induction decay occurs as the radiation at the three frequencies is turned off. At the sum frequency $\omega_F = \omega_1 + \omega_2 + \omega_3$ a coherent wave is generated by

$$\sigma_{da}(t) = (d|e^{-i\xi t_1}|a)(a|e^{i\xi t_1}|a)e^{i\Psi_{F\alpha}}, \tag{42}$$

where $\Psi_{F\alpha} = -\omega_{da}(t - t_1) + \sum \psi(t_1)$. Following the procedure which was used for Eqs. (20)–(22) the phase of the free-induction wave is given by Eq. (41a) for optical nutation and the Doppler term by $\Delta_{F\alpha} = -(\omega_{da} - \omega_F + \dot{\varphi}_{F\alpha})$. Averaging over $\dot{\varphi}_{F\alpha}$ for all terms yields the amplitude, and its dependence on the interval $t - t_1$. The effect of the decay times on the decay of σ_{da} is not apparent in our formulation.

If during this decay a probe signal[10–12] is turned on as discussed in Sec. II F, $\sigma_{da}(t')$ can be observed. All of the arguments of Sec. II F can be repeated. Thus

$$\sigma_{ba} = (b|e^{-i\xi s(t-t')}|d)\sigma_{da}(t')\,(a|e^{i\xi s(t-t')}|a)e^{i\Psi\alpha} \tag{43}$$

generates a coherent wave with phase $\varphi_1 - \omega_1 t$. The eikonal of interest is

$$\Psi_\alpha + \Psi_{F\alpha} - \psi_{1\alpha} = \psi_1^S(t) + \sum[\psi_n^i(t_1) - \psi_n^S(t')] - \omega_{da}(t' - t_1) - \psi_1(t).$$

Independence of position requires a phase of

$$\varphi_1 = \varphi_1^S + \sum(\varphi_n^I - \varphi_n^S). \tag{44}$$

The Doppler effect leads to a term of the type $[\omega_{da} - \omega_F + \sum \dot{\varphi}_n](t' - t_1)$. As an average is taken over $\dot{\varphi}_\alpha$ the amplitude at the interval $t - t'$ depends on $\sigma_{da}(t')$ and on a decay time typical of free-induction decay.

III. DISCUSSION

A general feature of photon echoes which are produced by stimulation of the nonlinear medium by three plane waves is shown in Fig. 3. The first pulse is a superposition of three noncollinear but coplanar waves with wave vectors $\vec{k}_1^I$, $\vec{k}_2^I$, $\vec{k}_3^I$. The second pulse is a superposition of three collinear plane waves $\vec{k}_n^{II}$. The wave vector $\vec{k}_n$ is at frequency ω_n. Equations (21a), (29), and (32) yield the echo directions. Equation (24) can be used for the echo direction at the sum frequency. For the small angles with the 3-direction which must be used these equations reduce to $\theta_E = -\sum \omega_n \theta_n / \omega_E$, where the second pulse is used as the reference direction and $\omega_E = \sum \omega_n$. The echo at the sum frequency $\omega_E = \omega_1 + \omega_2 + \omega_3$ is an electric dipole transition and occurs at the angle

$$\theta_E = -(\omega_1\theta_1 + \omega_2\theta_2 + \omega_3\theta_3)/\omega_E.$$

Echoes occur at angles $-\theta_1$, $-\theta_2$, $-\theta_3$, at frequencies ω_1, ω_2, ω_3. Quadrupole echoes occur at the sums of pairs and the echo at $\omega_1 + \omega_2$ occurs at $\theta_E = -(\omega_1\theta_1 + \omega_2\theta_2)/(\omega_1 + \omega_2)$, etc., for the other pairs. All of these possible echoes are shown in Fig. 3. Pulse duration and amplitudes can be used

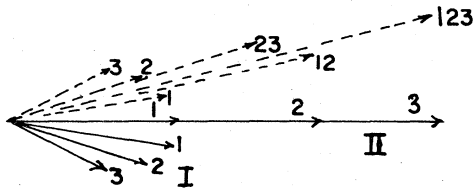

FIG. 3. Three plane-wave coplanar pulses with wave vectors $\vec{k}_1^I$, $\vec{k}_2^I$, $\vec{k}_3^I$ and three collinear plane wave pulses $\vec{k}_1^{II}$, $\vec{k}_2^{II}$, $\vec{k}_3^{II}$ form six plane-wave photon echoes with wave vectors $\vec{k}_E$ which follow from Eq. (24) and the gradient of Eqs. (29) and (32). Thus the echo at the sum frequency is given by $\vec{k}_E = \sum_m (2\vec{k}_m^{II} - \vec{k}_m^I)$ where the sum is over $m = 1, 2, 3$, at ω_1 with $m = 1$, at $\omega_1 + \omega_2$ with $m = 1$, 2, etc.

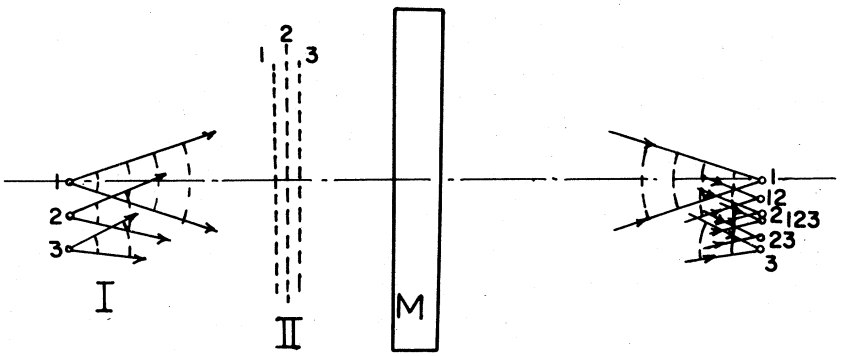

FIG. 4. Three diverging waves at ω_1, ω_2, ω_3 form the first pulse I and three plane waves form the second pulse II. The six photon echoes stimulated in the nonlinear medium M are converging waves and come to focus at the positions shown. 1 implies the photon echo at ω_1, 123 the photon echo at $\omega_1+\omega_2+\omega_3$, etc.

to enhance the intensity of a particular echo. As thick samples are considered, the phase matching condition which is expressed by Eq. (36) must be included. It should be noted that quadrupole matrix elements can be large. This occurs for the ^2D-^2S transition in Na.[14-17] The interaction strength depends on $(c|\vec{D}|a)\cdot\hat{k}$ and for noncollinear waves is nonzero. Even so the interaction is linear in θ and is quite small for the milliradian angles under consideration.

Photon echoes which are generated by spherical waves with centers of curvature x_n^{I}, y_n^{I}, z_n^{I} and x_n^{II}, etc., for the first and second pulses at frequency ω_n have a center of curvature which is given by Eqs. (34) and (35) for the echo at the sum frequency. If the sums over n are limited to one frequency these equations can be used for the echoes at ω_n. The sum over any two indices can be used for the echoes at $\omega_1+\omega_2$, etc. Since six echoes occur it is difficult to place this information on a figure similar to Fig. 3. For the special example of a second pulse which is composed of collinear plane waves and a first pulse which is composed of coplanar spherical waves Eqs. (34) and (35) reduce to $1/z_E=-[\sum\omega_n/z_n^{\mathrm{I}}]/\sum\omega_n$, and $x_E/z_E=-[\sum\omega_n x_n^{\mathrm{I}}/z_n^{\mathrm{I}}]/\sum\omega_n$. If diverging waves are used for the first pulse, then the echoes come to focus at $x_E=x_n^{\mathrm{I}}$, $z_E=-z_n^{\mathrm{I}}$ for ω_n; at the values of x_E and z_E which follow with $n=1,2$ for the echo at $\omega_1+\omega_2$, etc. An example is shown in Fig. 4 for a selected set of $\vec{k}_n$.

Since the general optics of optical nutation and free-induction decay are simpler than the optics for photon echoes, they are considered next. Equation (40) describes the effects at the sum frequency and yields a term for the electric polarization which is proportional to

$$v_1v_2v_3e^{i(\varphi_1+\varphi_2+\varphi_3)}e^{-i(\omega_1+\omega_2+\omega_3)t}.$$

If spherical waves at frequencies ω_n have centers of curvature x_n, y_n, z_n then the spherical wave generated at the sum frequency has a center of curvature x_N, y_N, z_N which is given by Eq. (41). Thus $1/z_N=\sum(\omega_n/z_n)/\omega_N$ and $x_N/z_N=\sum(\omega_n/\omega_N)(x_n/z_n)$, etc. for both optical nutation and free-induction decay. For more complex wave fronts a more careful analysis is needed.

In most of our discussion the source has been represented by $ve^{i\varphi}$ where v and φ are functions of x, y, z in the nonlinear medium. For multiple sources in the object plane it is convenient to use the Fresnel approximation and for the x-z plane this becomes

$$ve^{i\varphi}=e^{ik(z-z_0)}\sum_m v_m e^{ik(x-x_m)^2/2(z-z_0)}$$

near $z=0$ in the nonlinear medium. Each term in the sum is a suitable eikonal but now v can have a rapid spatial variation. The wave generated at the sum frequency is the triple product of the sums at each frequency. Each term in this triple sum is the same as the simple example of three sources and is equivalent to a virtual source at x_N, y_N, z_N for each set of x_n, y_n, z_n. Since the number of terms in the triple sum or the number of virtual sources increases at the product $N_1N_2N_3$, it is apparent that overlapping of virtual sources will occur as the number of sources in the object plane increases. This complex pattern may not be useful and can be avoided by making two of the three wave fronts, plane waves. Then for the third wave ω_n, one has for a simple source $z_N=(\omega_N/\omega_n)z_n$ and $x_N=x_n$. Superposition can be used to describe more complex wave fronts and yields a magnification of ω_n/ω_N at the sum frequency ω_N. This result is similar to that reached for two-wave mixing with crystals in parametric up-conversion. The steady-state component which has not been considered in our development has these same features for three-wave mixing.

Even in the example with two plane waves the wave front generated at the sum frequency need not be a good reproduction with magnification ω_n/ω_N. Both optical nutation and free-induction decay are transient phenomena and as the matrix elements of $e^{i\Xi t}$ are evaluated in Eqs. (40) or (42) the effects of saturation are apparent in the roots

λ_m. Saturation occurs in the resonant example which is described by Eq. (26). The amplitude oscillates as τ varies and the magnitude of the matrix element cannot exceed unity. Thus the amplitude of the generated wave front may be poorly related to the amplitude in the object plane.

Other optical arrangements can be used. A source or object can be formed by illumination with one of the three frequencies. If a converging lens is placed a focal distance f from the object, then the transverse Fourier transform

$$v e^{i\varphi} = e^{ik(z-f)} \sum_m v_m e^{-ik(x_m/f)x}$$

occurs in the nonlinear medium at a distance f after the lens. A beam splitter can be used to mix the parallel beams at the other two frequencies with the Fourier transform. An image can now be formed by placing a second lens of focal length f' a distance f' after the nonlinear medium, and then a magnification $\omega_n f'/\omega_N f$ occurs for the radiation at the sum frequency. Firester[7] has discussed the optical advantages of this arrangement for a thick nonlinear medium for parametric up conversion with two frequencies.

The comments just made for optical nutation and free-induction decay for the more complex wave fronts are applicable to photon echoes. The spatial dependence of the amplitude in the nonlinear medium is a limiting feature for transient effects. For this reason the discussion is now limited to waves which undergo phase distortion along their optical paths. Thus a plane wave undergoes the deformation

$$v e^{ikz} \rightarrow v e^{i\kappa(x,y,z)} e^{ikz}$$

as it passes through an almost transparent medium. The amplitude is almost constant and for a near nonlinear medium remains almost constant. The dominant feature is the phase and these phases can be added in the sense which is given by Eqs. (21a), (29), (32) for photon echoes, Eqs. (39b) and (44) for new pulses, and Eq. (41a) for optical nutation and free-induction decay. For the photon echo formed by a single frequency the phase conjugate or with a suitable optical arrangement the phase conjugate of the Fourier transform can be formed. More generally the transverse phases can be changed to $2\kappa^{II} - \kappa^{I}$.

Since the gradient of the phase yields the wave vector or the wave normal, the gradient of Eq. (21a) yields Eq. (24) where the $\vec{k}_n$ are now functions of x, y and this yields some information about the echoes generated by more than one frequency. This same concept can be used for the generation of a new pulse which was discussed in Sec. II F. The wave vector of the new pulse follows from the gradient of Eq. (39b) and at each x, y in the sample $\vec{k}_1$ for the new pulse is

$$\vec{k}_1 = -(\vec{k}_2^S + \vec{k}_3^S) + 2(\vec{k}_1^{II} + \vec{k}_2^{II} + \vec{k}_3^{II}) - (\vec{k}_1^{I} + \vec{k}_2^{I} + \vec{k}_3^{I}) .$$

The photon echo at ω_1 and the new pulse at ω_1 can have different directions. This equation describes the two-frequency effects which were previously suggested[11] with $k_3 = 0$. With plane waves and $\vec{k}_1^{I} = \vec{k}_1^{II}$ and $\vec{k}_2^{I} = \vec{k}_2^{II}$, the single-frequency photon echoes occur along either $\vec{k}_1$ or $\vec{k}_2$. The sum frequency or quadrupole echo occurs along $\vec{k}_1 + \vec{k}_2$ but is too weak to observe. A probe pulse $\vec{k}_2^S$ yields a new pulse with $\vec{k}_1 = -\vec{k}_2^S + \vec{k}_1 + \vec{k}_2$. Both the single-frequency echoes and the "two-photon echo" or probe-pulse echo have been observed. Phase-matching conditions favor the probe-pulse echo as the angle between $\vec{k}_1$ and $\vec{k}_2$ increases.

If the first and second pulses are collinear plane waves and the probe pulse described by $\varphi^S = \kappa_2 + k_2 z$, then the new pulse has a phase $\varphi_1 = -\kappa_2 + k_1 z$ and is in a sense the phase conjugate of the probe pulse. For three waves the new pulse has a phase $\varphi_1 = (\kappa_2 + \kappa_3) + k_1 z$ and depends on the sum of the phases and generates a wave which in a sense is the conjugate of these two waves. If in Fig. 2 a probe pulse is turned on after the first pulse then a new pulse is generated and by Eq. (44) at each x, y in the thin sample $\vec{k}_1 = \vec{k}_1^{I} + \vec{k}_2^{I} + \vec{k}_3^{I} - \vec{k}_2^S - \vec{k}_3^S$.

In conclusion one can add and subtract the transverse phases κ in single-frequency photon-echo and Carr-Purcell photon-echo experiments for waves with almost constant amplitude. For pulses at two and three frequencies similar addition and subtraction operations are possible for photon echoes and probe-pulse echoes. A useful application which is known as phase adaptive occurs when linear superposition can be used. It is with some regret that the authors cannot present a general use for the novel feature of being able to add and subtract the phases of wave fronts.

---

[1]A. Yariv, Appl. Phys. Lett. 28, 88 (1976); Opt. Commun. 21, 49 (1977).
[2]R. W. Hellwarth, J. Opt. Soc. Am. 67, 1 (1977).
[3]C. V. Heer and P. F. McManamon, Opt. Commun. 23, 49 (1977).
[4]C. V. Heer, Phys. Rev. A 7, 1635 (1973).
[5]D. M. Bloom and G. C. Bjorklund, Appl. Phys. Lett. 31, 592 (1977); P. V. Avizonis, F. A. Hopf, W. D. Bomberger, S. F. Jacobs, A. Tomita, and K. Womack, *ibid.* 31, 435 (1977); D. M. Pepper, D. Fekete, and

A. Yariv, *ibid.* 33, 41 (1978); P. F. Liao, D. M. Bloom, and N. P. Economou, *ibid.* 32, 813 (1978); E. E. Bergmann, I. J. Bigio, B. J. Feldman, and R. A. Fisher, Opt. Lett. 3, 82 (1978); D. M. Bloom, P. F. Liao, and N. P. Economou, *ibid.* 2, 58 (1978); unpublished papers on CS_2, Na, and Ge were given at the Tenth International Quantum Electrons Conference.

[6]N. C. Griffen and C. V. Heer, Appl. Phys. Lett. 33, 865 (1978).

[7]See A. H. Firester, J. Appl. Phys. 41, 703 (1970); F. Zernike and J. E. Midwinter, *Applied Nonlinear Optics* (Wiley, New York, 1973), for a discussion and reference to earlier work.

[8]C. V. Heer, Phys. Rev. A 13, 1908 (1976).

[9]S. R. Hartmann, IEEE J. Quantum Electron. 4, 802 (1968); see also M. Aihara and H. Inaba, J. Phys. A 6, 1709, 1725 (1973); T. M. Makhiviladze and M. E. Sarychev, Zh. Eksp. Teor. Fiz. 69, 1594 (1975) [Sov. Phys. JETP 42, 812 (1973)]; S. Aoki, Phys. Rev. A 14, 2258 (1976); H. Hatanaka and T. Hashi, J. Phys. Soc. Jpn. Lett. 39, 1139 (1975).

[10]P. Hu, S. Geschwind, and T. M. Jedju, Phys. Rev. Lett. 37, 1357 (1976); 37, 1773(E) (1976).

[11]A. Flusberg, T. Mossberg, R. Kachru, and S. R. Hartmann, Phys. Rev. Lett. 41, 306 (1978).

[12]P. F. Liao, J. E. Bjorkholm, and J. P. Gordon, Phys. Rev. Lett. 39, 15 (1977).

[13]B. R. Mollow, Phys. Rev. 188, 1969 (1969); Phys. Rev. A 2, 76 (1970); 13, 758 (1976); H. J. Kimble and L. Mandel, *ibid.* 13, 2123 (1976).

[14]D. S. Bethune, R. W. Smith, and Y. R. Shen, Phys. Rev. Lett. 38, 647 (1977); 37, 431 (1976); Phys. Rev. A 17, 277 (1978).

[15]C. E. Tull, M. Jackson, R. P. McEachran, and M. Cohen, Can. J. Phys. 50, 1169 (1972).

[16]It is often overlooked that some quadrupole transitions are extremely strong. There is experimental evidence that the $3d\,^2D$-$3s\,^2S$ quadrupole transition in Na is somewhere between $\frac{1}{4}$ and $\frac{1}{100}$ as intense as the electric dipole Na-*D* lines in emission. [See A. N. Zaidel', V. K. Prokof'ev, S. M. Raiskii, V. A. Slavnyi, and E. Ya. Shreider, *Tables of Spectral Lines* (Plenum, New York, 1970); and A. R. Striganov and N. S. Sventitskii, *Tables of Spectral Lines of Neutral and Ionized Atoms* (Plenum, New York, 1968) for an estimate of line intensities.] These references indicate that the $3d\,^2D$-$3s\,^2S$ transition is comparable to the $3d\,^2D$-$3p\,^2P$ electric dipole transition. The Theoretical calculations of Tull *et al.* (Ref. 15) indicate a large quadrupole matrix element for these transitions, but not nearly as large as the tabulated data. Their value (Ref. 15) was used in recent experiments, and Bethune *et al.* (Ref. 14) suggest that these matrix elements yield reasonable agreement with experimental data. No direct measurement is available.

[17]A. Flusberg, T. Mossberg, and S. R. Hartmann, Phys. Rev. Lett. 38, 59 (1977); M. Matsuoka, H. Nakatsuka, H. Uchiki, M. Mitsunaga, *ibid.* 38, 894 (1977).